

## **SLR2000 Closed Loop Tracking with a Photon-Counting Quadrant Detector**

**Jan McGarry  
Thomas Zagwodzki  
John Degnan**

**NASA / Goddard Space Flight Center  
Greenbelt, Maryland 20771 USA**

### Abstract:

*SLR2000 will close the tracking loop using a Photek four quadrant Micro-Channel Plate (MCP) detector which will provide information to correct the along-track, ranging, and cross-track errors automatically in realtime. Analysis and simulation results showing the expected performance of this loop will be presented and will take into account the recent test results of the Xybion mount's tracking abilities. The details of the full tracking loop (both uplink and downlink) will also be given.*

### Introduction

SLR2000 will be a completely autonomous satellite laser tracking / ranging system [Degnan 1998]. Current NASA Satellite Laser Ranging (SLR) systems require an operator to determine if the target has been acquired, to optimize the pointing, and to maintain tracking. On SLR2000 a Photek four quadrant Micro-Channel Plate (MCP) detector will provide the information to allow the software to determine if the satellite has been acquired, to correct the telescope pointing, and to provide both along-track and cross-track corrections in realtime.

The important parts of the Tracking Loop are pictured in Figure 1 along with the current SLR2000 facility. A simplified block diagram of the system is shown in Figure 2. The outgoing laser pulse passes through a Risley Prism pair which controls a two-angle point-ahead offset from the telescope pointing. A small portion of the outgoing laser pulse is sampled and input to the Event Timer which records the transmit time. The telescope is pointing along the path of the returning light (the receive path). The satellite returns pass through the passive transmit /receive switch and through the spatial filter to the four quadrant micro-channel plate (4QMCP) PMT. The return times are measured at the Event Timer and also tagged to indicate the quadrant. A zoom provides the ability to change both the system divergence and the receiver field of view by a factor of 4 (from 10 to 40 arcseconds).

The SLR200 system specifications relevant to the tracking loop are given in Figure 3.

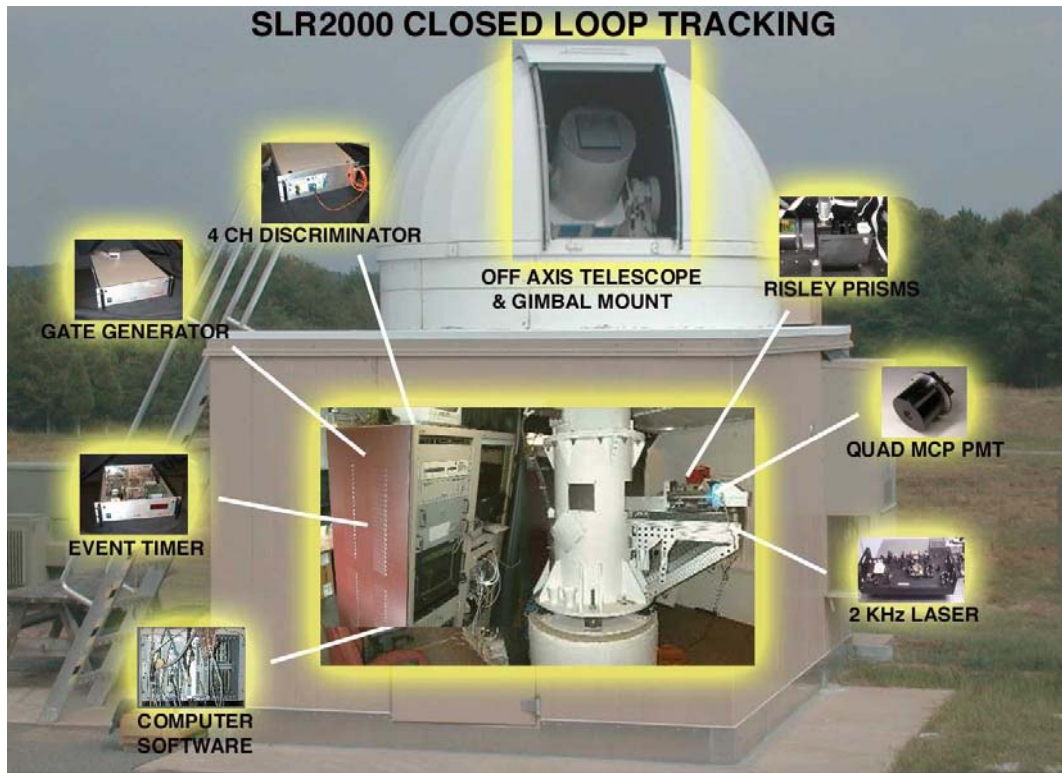


**Figure 1: SLR2000 System**

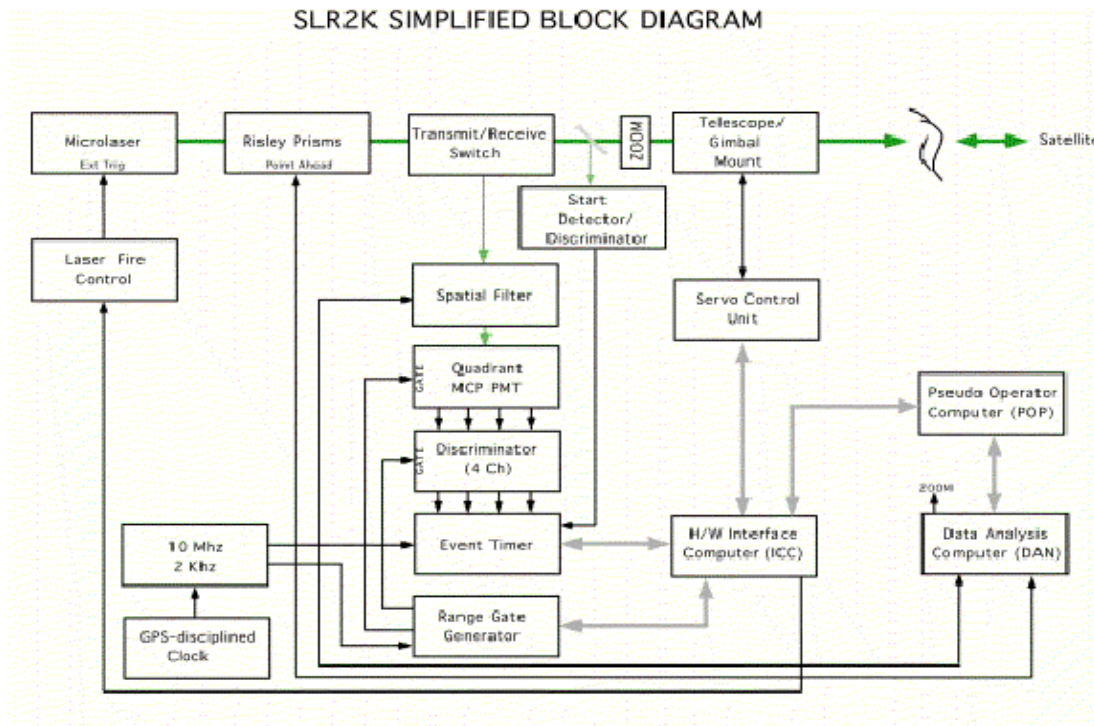


**Figure 2: SLR2000 Block Diagram**

### SLR2K TRACKING SYSTEM SPECIFICATIONS

|                        |   |
|------------------------|---|
| <b>Laser:</b>          | <b>Diode pumped Nd:YAG OSC/AMP</b>        |
| <b>Fire rate:</b>      | <b>2 KHz</b>                              |
| <b>Pulse Energy:</b>   | <b>135 ujoules/pulse at exit aperture</b> |
| <b>Beamwidth:</b>      | <b>Variable: 10 to 40 arcsec</b>          |
| <b>Detector:</b>       | <b>Photek quadrant MCP PMT</b>            |
| <b>Gain:</b>           | <b>3.E6</b>                               |
| <b>QE:</b>             | <b>13% @ 532 nm</b>                       |
| <b>Active area:</b>    | <b>12 mm diameter</b>                     |
| <b>Image size:</b>     | <b>6 mm</b>                               |
| <b>Receiver:</b>       | <b>4 independent channels</b>             |
| <b>Field of view:</b>  | <b>Step Variable: 10 to 40 arcsec</b>     |
| <b>Discriminator:</b>  | <b>Phillips Scientific 708</b>            |
| <b>TIU:</b>            | <b>HTSI 1.5 ps Resolution ET</b>          |
| <b>Risley prisms:</b>  | <b>0-30 arcsec transmit point ahead</b>   |
| <b>T/R Switch:</b>     | <b>Passive (Polarization insensitive)</b> |
| <b>Telescope:</b>      | <b>OSC 40 cm off-axis</b>                 |
| <b>Tracking Mount:</b> | <b>Xybion Az/EI gimbal</b>                |
| <b>Tracking error:</b> | <b>~ 1 arcsec RMS both axes</b>           |
| <b>Command rate:</b>   | <b>50 Hertz</b>                           |

**Figure 3: SLR2000 Tracking System Specifications**

#### Details of the Transmit and Receive Paths

Because of the spacecraft motion with respect to the station, there is a small angular difference between the pointing angles required to transmit the laser light, and the pointing angles required to center the return light in the receiver field of view. The pointing angles needed to transmit the laser pulse (point-ahead) are calculated using the satellite position at the time the current outgoing laser pulse will reach the satellite. Similarly the angles required to receive the return pulses (point-behind) are calculated for the satellite position when the current incoming laser pulse left the satellite. Due to the high repetition rate of the laser SLR2000 will have between a few to many hundred fires in flight at any given time.

Unlike conventional SLR systems, due to its narrow laser divergence and narrow field of view, SLR2000 must separately point both the transmit and the receive in order to simultaneously place the center of the transmit pulse on the satellite and keep the returns within the receiver field of view. The telescope is used to point the receiver along the return light path. The quadrant detector input is used by the software in a closed-loop calculation

to center the returns by biasing the telescope pointing.

Two Risley Prisms are used to offset the transmit beam from the telescope. This transmit pointing is accomplished completely open-loop by a geometric calculation using the satellite position and velocity vectors, and the station position.

Since all of the transceiver optics and controls are on the optical bench below the telescope, the effects of the Coude Path Rotation must be corrected for in both the Risley Prism command angles and in the quadrant detector implied telescope bias corrections.

Figure 4 gives a summary of the transmit and receive sections of the tracking loop.

| <b><u>TRANSMIT</u></b>  | <b><u>RECEIVE</u></b>  |
|---|--|
| <ul style="list-style-type: none"><li>- Laser beam is offset pointed ahead from telescope (two-angle offset).</li><li>- Risley Prisms used to steer beam completely open-loop.</li><li>- Outgoing beam orientation is affected by Coude Path Rotation.</li><li>- Maximum offset from receive path for earth rotating satellites is 11 arcseconds.</li></ul> | <ul style="list-style-type: none"><li>- Telescope points behind - to location where last return is coming from.</li><li>- Closed-loop using 4QMCP.</li><li>- Return image is affected by Coude Path Rotation.</li><li>- Field of view is 10 arcseconds to 40 arcseconds.</li></ul> |

**Figure 4: Table of SLR2000 Transmit / Receive Characteristics**

Figure 5 details the 40 cm off-axis SLR2000 telescope built by Orbital Science Corporation (OSC) and the elevation over azimuth gimbal mount built by Xybion Corporation. Pointing mount and telescope protrude through the shelter roof into the dome area supported by the riser pedestal. Five flat mirrors of enhanced aluminum direct the two inch diameter collimated beam through the gimbal to the eyepiece lens where it is expanded to fill the secondary and primary mirrors. Anti-reflective coated entrance and exit windows on both the gimbal and telescope prevent contamination from dust and moisture and eliminate airflow. Slip rings in azimuth permit continuous azimuth rotation while elevation is limited from 0 to 180 degrees movement.

The transceiver table with the laser transmitter, receiver, boresighting cameras, and all transmit receive optics are shown in Figure 6. Laser output is expanded and injected into the azimuth axis of the gimbal while the return photons are split off and directed to the QMCP PMT. The transmit/receive switch is a passive polarization insensitive device which directs all receive photons into the receive path while enabling passage of the laser pulse out of the system. This is done with a polarizing splitter and combiner. All return photons are focused onto the photocathode of the QMCP PMT with the accumulation of counts in each quadrant determining satellite location in the far field. The mount is driven to minimize pointing errors as determined by the return count in the QMCP PMT. Boresighted with the laser transmitter and receive PMT is a CCD camera for star calibrations. An additional optical path via flip mirror supports a second CCD camera with larger field of view and an eyepiece.

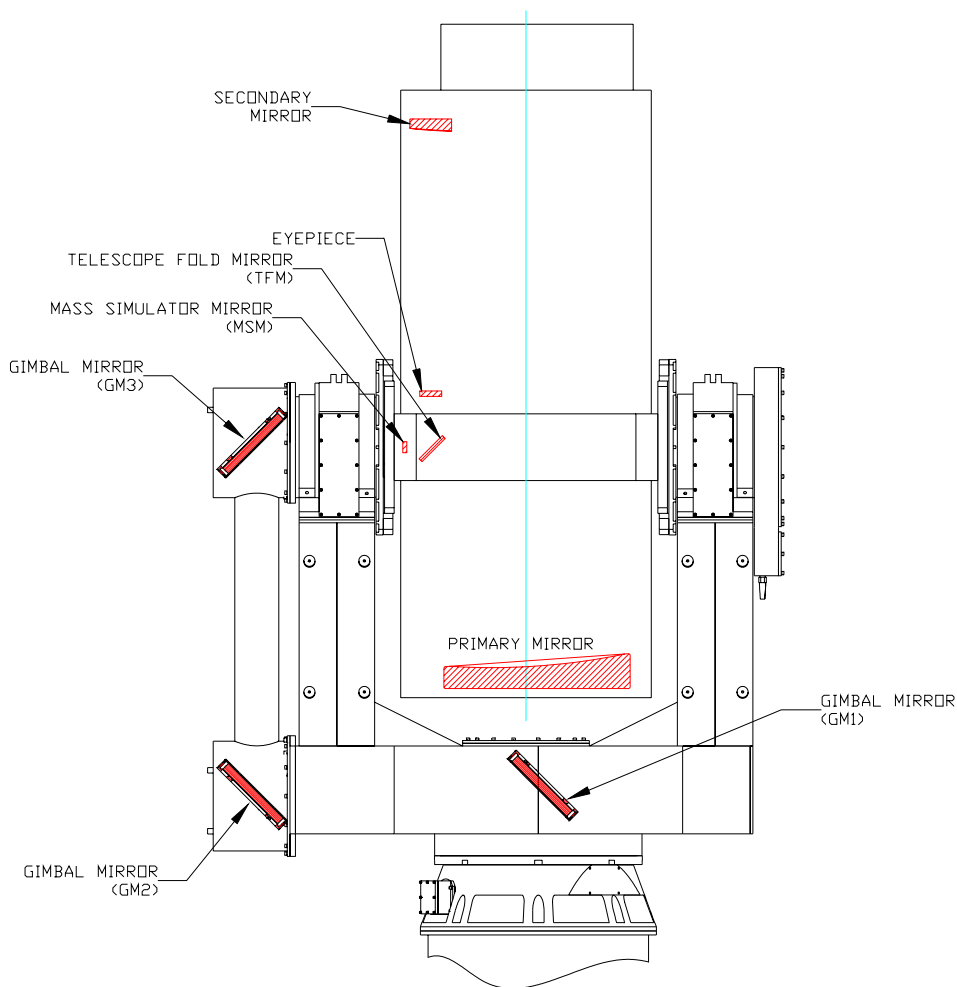


**Figure 5: SLR2000 Telescope and Gimbal**

### **Figure 6: Tranceiver Optical Bench**

#### Open-Loop Transmit Point Ahead

The telescope points the receiver to the satellite's position when the light from the current incoming return left the retroreflector. This is shown in Figure 7 as  $R_B$ . The Risley Prisms offset point the outgoing laser beam along  $R_A$  which points to the satellite's location at the time the light will reach the spacecraft.

The angular offset in the orientation of one Risley Prism with respect to the other provides the magnitude of the angular offset ( $Rho$ ). The rotation of the pair from a reference provides the angular orientation of the  $R_A$  vector about the  $R_B$  vector.

Specifically the two angle point-ahead offset is:

$$\cos(\rho) = \vec{R}_A \cdot \vec{R}_B / |\vec{R}_A| \cdot |\vec{R}_B|$$

$$\cos(\beta) = \vec{R}_0 \cdot (\vec{R}_A - \vec{R}_B) / (|\vec{R}_0| \cdot |\vec{R}_A - \vec{R}_B|)$$

which equivalently can be written as:

$$\rho = \sqrt{(\Delta Az)^2 \cdot \cos(El)^2 + (\Delta El)^2}$$

$$\beta = \tan^{-1}(\Delta Az \cdot \cos(El) / \Delta El)$$

where:

$\rho$  = Magnitude Angle (0 - 11 arcsec),

$\beta$  = Orientation Angle (0-360 deg),

$\Delta Az$ ,  $\Delta El$  = difference between point ahead and behind command angles (azimuth, elevation).

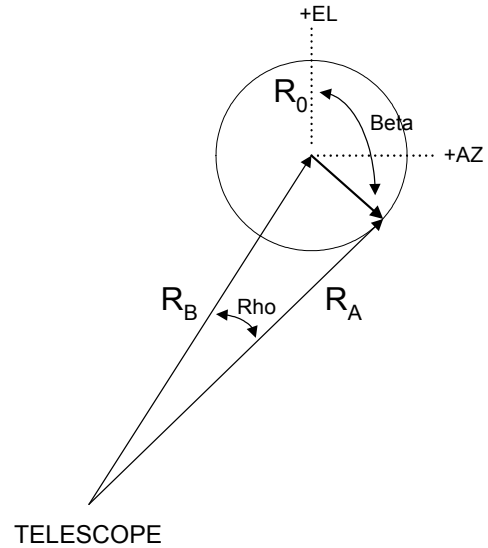


**Figure 7: Point Ahead Angles**

The maximum offset for earth orbiting satellites tracked by satellite laser ranging systems is 11 arcseconds. Some examples of the maximum value of the Magnitude (Rho) for various satellite altitudes are given in Figure 8. The Magnitude (Rho) depends upon the orientation of the orbit with respect to the station, the distance of the station to the satellite, and the velocity of the spacecraft with respect to the station. Although they are lower in altitude, the Low Earth Orbiting (LEO) satellites have higher maximum values for Rho due to their higher orbital velocities. A plot of the angles for a simulated 1000 km orbit is shown in Figure 9. Rho behaves similarly to the telescope elevation and the orientation angle (Beta) behaves similarly to the azimuth.

| Altitude (km) | Max EI (deg) | Max Rho (arcsec) |
|---------------|--------------|------------------|
| 300           | 45           | 10.6             |
| 400           | 81           | 10.5             |
| 1000          | 85           | 10.1             |
| 6000          | 82           | 7.8              |
| 20000         | 85           | 5.4              |

**Figure 8: Examples of the maximum value of the “magnitude” point-ahead angle**

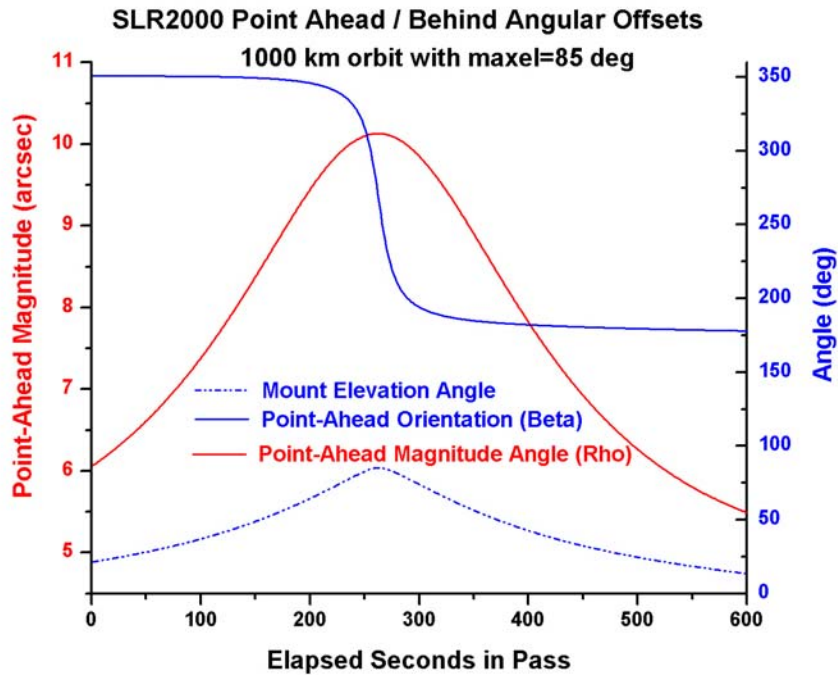


**Figure 9: Plot of the two Point-Ahead angles for a 1000km circular orbit**

### Receiver Control using Quadrant Detector

The flow of data from the four quadrant MicroChannel Plate Photomultiplier to the calculated angular biases used to control the mount, is shown in Figure 10. The range measurement is tagged with the number of the quadrant that recorded the return. The range data is then processed to determine the signal, independent of quadrant information [McGarry 1996]. The signal range data then goes into the calculation of Range Bias and Time Bias.

As a parallel process, the number of signal range measurements for each quadrant are counted. These counts are used to calculate a vector in receive space. This vector is then transformed into angular biases used to control the telescope. Before these angular biases can be used, however, they must have the Time Bias contribution from the signal range processing removed (since this bias was calculated from the same data).

The receive space vector is formed in the following manner:

$$\begin{aligned}
 N &= nQ1 + nQ2 + nQ3 + nQ4 \\
 dx &= [ (nQ1+nQ3) - (nQ2+nQ4) ] / NQ \\
 dy &= [ (nQ3+nQ4) - (nQ1+nQ2) ] / NQ
 \end{aligned}$$

where  $nQ1, nQ2, nQ3, nQ4$  are the signal return counts per quadrant.

For SLR2000 the Coude Path Rotation through the telescope optics is:

$$\theta = AZ - EL + 22.5 \text{ (degrees).}$$

A negative rotation about  $\theta$  to get  $(dx', dy')$ , followed by scaling, produces the telescope biases:

$$Az_{bias} = -dx' \cdot r_s / \cos(\text{elevation})$$

$$El_{bias} = -dy' \cdot r_s$$

where  $r_s \approx$  radius of return spotsize in field of view.

When the image is centered, the expected angular error due to the Poisson random process, is a function of the return spotsize and the total number of signal counts, and decreases as the total signal count increases:

$$\Delta \alpha \approx \frac{2 \cdot r_s}{\sqrt{N}}$$

When the spotsize is 2.5 arcseconds, to get the angular error below 1 arcsecond, the count will have to be  $\geq 25$ . The time to accumulate 25 returns depends upon the satellite altitude, elevation with respect to the station, and retroreflector lidar cross section. Typical times for a clear atmosphere at 20 degrees elevation are  $\sim 0.1$  seconds for STARLETTE,  $\sim 2.0$  seconds for LAGEOS, and  $\sim 7.0$  seconds for ETALON [Titterton 1996].

### How Mount Performance Affects 4QMCP Closed Loop Tracking

The RMS of the angular tracking errors, calculated over a 1 second period, for the Xybilon gimbal are generally at or below the 1 arcsecond level [Patterson 2002]. The raw tracking data, however, shows many arcseconds of random errors with distinct periodic fluctuations at 1 Hz, 2Hz, and above, which tend to have higher amplitudes at the higher angular velocities (2-5 deg/sec). Figure 11 shows the elevation raw tracking errors for a 5 deg/sec velocity test performed in February 2002 at Goddard's Geophysical and Astronomical Observatory.

Monte Carlo simulations were performed to determine the accuracy of the telescope biases calculated in the presence of the tracking errors. The location of the return image on the detector was determined by differencing the instantaneous mount pointing with the known satellite location. The relative area of the image in each quadrant was then determined. The probability for getting a signal return was assigned to each quadrant as a function of the satellite lidar link equation [Degnan 1993] and the percentage of image area in that quadrant. Noise returns had equal probabilities for each quadrant which were based upon the combination of instrument noise and optical background noise. A Bernoulli trial was run for each laser fire to determine if there would be a signal return, a noise return, or no return, and if there was a return, which quadrant it would be in. The tracking performance was simulated by combining two random processes with periods of 1 Hz and 2 Hz respectively.

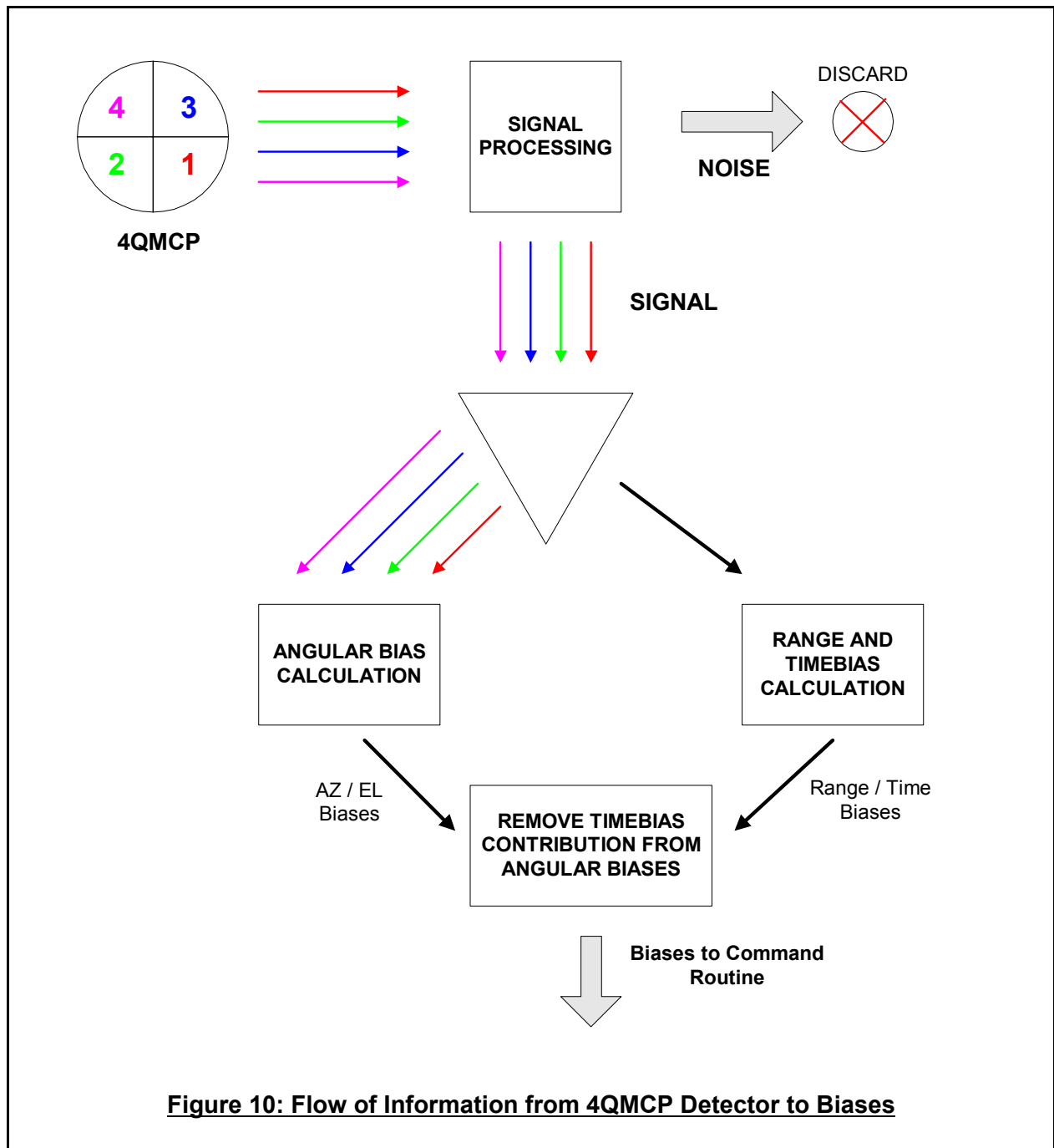
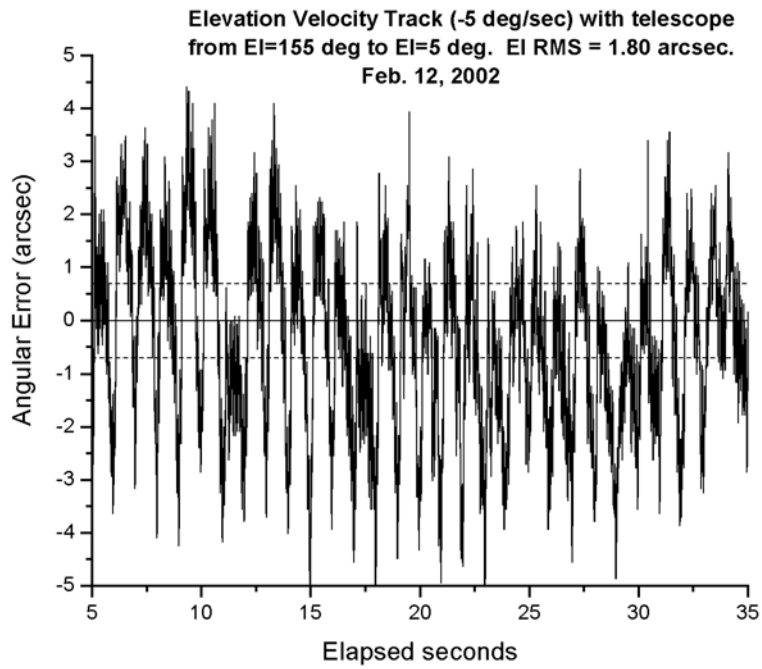
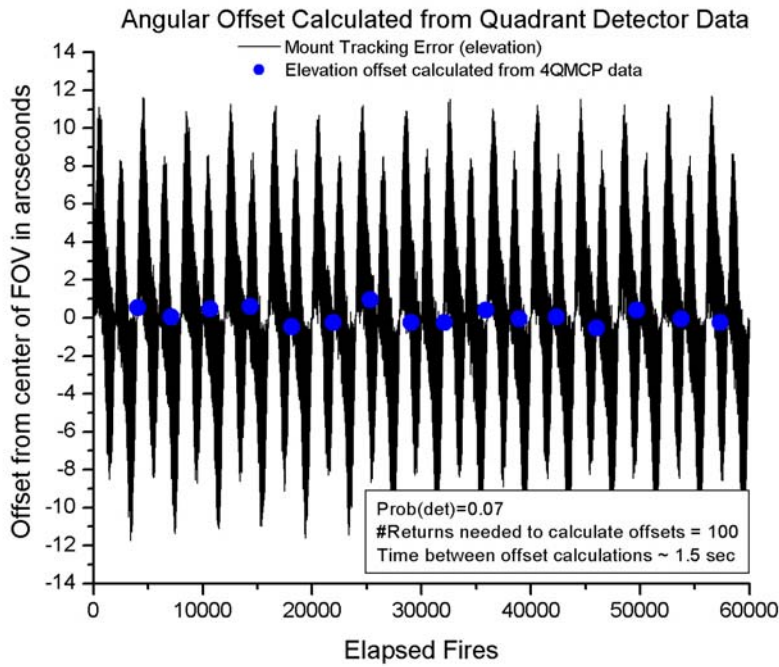


Figure 12 shows the simulated mount performance and the elevation biases calculated in the presence of these mount errors, using the process shown in Figure 10. If the quadrant information is integrated over a period longer than 1 second, the biases calculated from the simulated information are in general accurate to within  $\pm 1$  arcsecond. Since the fluctuations in our simulated data tend to be more regular than in the real data, the results from our testing so far can only hint at the real performance.



**Figure 11: Actual Tracking Performance from Xybio Mount Testing.  
Elevation Velocity Track (-5 degrees/sec) - February 12, 2002.**



**Figure 12: Simulated Tracking Performance with Calculated Biases Superimposed.**

## Conclusions

It appears that quadrant detector information can still effectively be used to close the tracking loop on SLR2000, despite the raw mount tracking performance, due to the periodic nature of the tracking errors. If the integration time is chosen to be long enough (> 1 second), simulations suggest that the tracking errors average out.

The open loop point-ahead has never been tried, to the author's knowledge, on any satellite laser ranging systems, and so the Point-Ahead calculation and Risley Prism offsets need to be verified during actual SLR2000 satellite tracking.

## References

Degnan, J., 1993, "Millimeter accuracy satellite laser ranging: a review," in D.E. Smith and D.L. Turcotte (eds), *Contributions of Space Geodesy to Geodynamics: Technology*, AGU Geodynamics Series, Vol.25, pp.133-162.

Degnan, J., 1998, "SLR2000 Project: Engineering Overview and Status", *Proceedings of 11<sup>th</sup> International Workshop on Laser Ranging*, Deggendorf, September 20-15, pp.389-395.

McGarry, J., 1996, J. Degnan, P. Titterton, et al, "Automated tracking for advanced satellite laser ranging systems," *SPIE Proceedings on Acquisition, Tracking and Pointing X*, Vol. 2739, April 10-11, Orlando, Florida, pp.89-103.

Patterson, D., 2002, and J. McGarry, "Overview of Data for the SLR2000 Tracking Mount Performance Testing," in this Proceedings.

Titterton, P., 1996, and H. Sweeney, "Correlation Processing Approach for Eyesafe SLR2000," *Proceedings of 10<sup>th</sup> International Workshop on Laser Ranging*, Shanghai, November, pp.378-384.